PHYSICAL REVIEW B, VOLUME 64, 020403(R)

X-ray magnetic circular dichroism study of $TbNi_2B_2C$

C. Song,[1] J. C. Lang,[2] C. Detlefs,[3] A. Létoublon,[1] W. Good,[1] J. Kim,[1] D. Wermeille,[1] S. L. Bud'ko,[1] P. C. Canfield,[1] and A. I. Goldman[1]

[1]*Ames Laboratory–US DOE and Department of Physics and Astronomy, Iowa State University, Ames, Iowa 50011*

[2]*Advanced Photon Source, Argonne National Laboratory, Argonne, Illinois 60439*

[3]*European Synchrotron Radiation Facility, Boîte Postale 220, 38043 Grenoble Cedex, France*

(Received 22 March 2001; published 15 June 2001)

X-ray magnetic circular dichroism measurements were performed on $TbNi_2B_2C$ in order to confirm the weak ferromagnetism reported for this material at low temperatures. Below approximately 8 K, an increase in the dichroic signal was observed at the Tb L_{III} edge, consistent with the onset of weak ferromagnetism involving the Tb ions. At an external magnetic field of 500 G, the ferromagnetic order parameter was obtained, and is in good agreement with the bulk magnetization data measured by a SQUID magnetometer.

DOI: 10.1103/PhysRevB.64.020403 PACS number(s): 75.25.+z, 75.50.−y, 75.30.−m, 75.30.Cr

Great interest in the RNi_2B_2C (R=rare earth) family continues because of the rich variety of ground state physical properties of these compounds.[1–5] In particular, there have been numerous investigations of the relationship between the competing interactions of superconductivity and long range magnetic order.[6] Recently, for example, the onset of weak ferromagnetism in $ErNi_2B_2C$ ($T_{WFM}\sim 2.5$ K) concomitant with the superconducting state ($T_c\sim 10$ K) was reported (Ref. 7), along with an upturn of the critical current with the onset of ferromagnetism, contrary to expectations.[8]

While $TbNi_2B_2C$, is not superconducting down to 7 mK (Ref. 9), it is closely related to the Er compound not only in its bulk thermodynamic properties,[10,11] but also in its microscopic magnetic ordering behavior.[12–15] Both systems order in an incommensurate spin wave along the [100] direction of the orthorhombic unit cell ($a>b$), with the magnetic moments confined to the basal plane. For both $TbNi_2B_2C$ and $ErNi_2B_2C$, the magnetic transition is accompanied by a lattice distortion from tetragonal symmetry (above T_N) to orthorhombic symmetry (below T_N). Perhaps most interestingly, similar lock-in transitions have been observed in both of these compounds in recent high resolution resonant magnetic x-ray scattering experiments.[16] The lock-in of the modulation wave vector to a commensurate value appears at the same temperature ($T_{WFM}\sim 8$ K) as the onset of weak ferromagnetism indicated by bulk susceptibility measurements.[10,7] Previous unpolarized neutron scattering experiments observed an increase in scattering consistent with weak ferromagnetism below approximately 8 K.[18] However, the magnetic origin of this additional scattering can only be verified by polarization analysis. Furthermore, ^{57}Fe Mössbauer and μSR experiments have indicated the onset of weak ferromagnetism through a reduction in the hyperfine field and the electronic spin fluctuation rate below T_{WFM}.[19]

In this paper, we report on recent x-ray magnetic circular dichroism (XMCD) experiments on $TbNi_2B_2C$ designed to directly probe the onset of a ferromagnetic component below T_{WFM} associated with the Tb ions. An XMCD experiment probes the difference, $\mu_c=(\mu^+-\mu^-)/(\mu^++\mu^-)$, in the absorption of x rays by a sample with the magnetic moment parallel (μ^+) and antiparallel (μ^-) to the helicity of the incident photon beam. Since the absorption involves transitions from well-understood core levels with well defined angular momentum, the observed structure in the dichroic signal can yield information about the spin polarization and spin-orbit coupling of the final states.[17] The information obtained from this measurement is element specific since the absorption measurement is made as the incident energy is scanned through an absorption edge. For the case at hand, the dichroic signal was measured at the Tb L_{III} absorption edge, corresponding to transitions from the Tb $2p_{3/2}$ core level to the spin-polarized $5d$ bands. Although the determination of the magnitude of the ferromagnetic moment using this method is very complicated, the dichroic signal scales directly with the ferromagnetic moment and can be used to confirm the existence of weak ferromagnetism in $TbNi_2B_2C$ associated with the Tb ions.

The x-ray magnetic circular dichroism experiment was carried out on the 6-ID undulator beamline of the MUCAT sector at Advanced Photon Source. A bent mirror was inserted after the double crystal Si(111) monochromator to eliminate higher harmonics of the incident beam. Control of the beam polarization was enabled using a thin diamond crystal phase retarder[20] to flip the incident σ polarized beam between left circularly polarized (LCP) and right circularly polarized (RCP) radiation. The dichroism measurements were done in a transmission geometry using a fine-grained powder sample produced by grinding single crystals similar to those used in earlier measurements.[10] The powder was uniformly spread on cellophane tapes and then combined to yield the change in absorption across the edge to be about one absorption length. The prepared sample was mounted on the cold finger of a helium cryostat equipped with superconducting magnet. By pumping on a JT-valve, sample temperatures down to 3 K in fields up to 40 kG could be reached.

Two different methods of data acquisition in XMCD experiments are possible. First, the direction of the magnetic field on the sample can be held constant while the beam polarization is flipped between positive (LCP) and negative helicity (RCP). Alternatively, the incident beam helicity can be held fixed while the magnetic field direction is reversed. Anticipating a small dichroic signal arising from weak ferromagnetism, data were obtained by combining both methods:

 ©2001 The American Physical Society

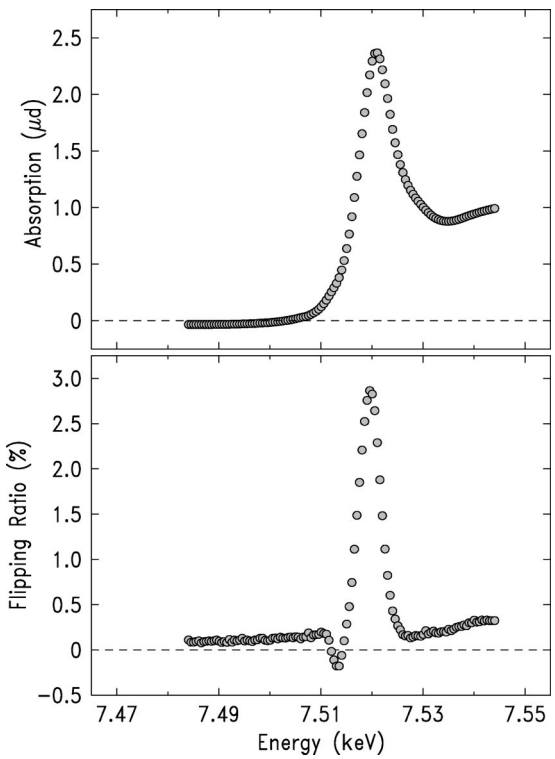

FIG. 1. Tb L_{III}-edge absorption (upper panel) and XMCD signal (lower panel) taken at $T=3.1$ K and $H=40$ kG on $TbNi_2B_2C$. For both panels, circles show the averaged value from flipping the external field.

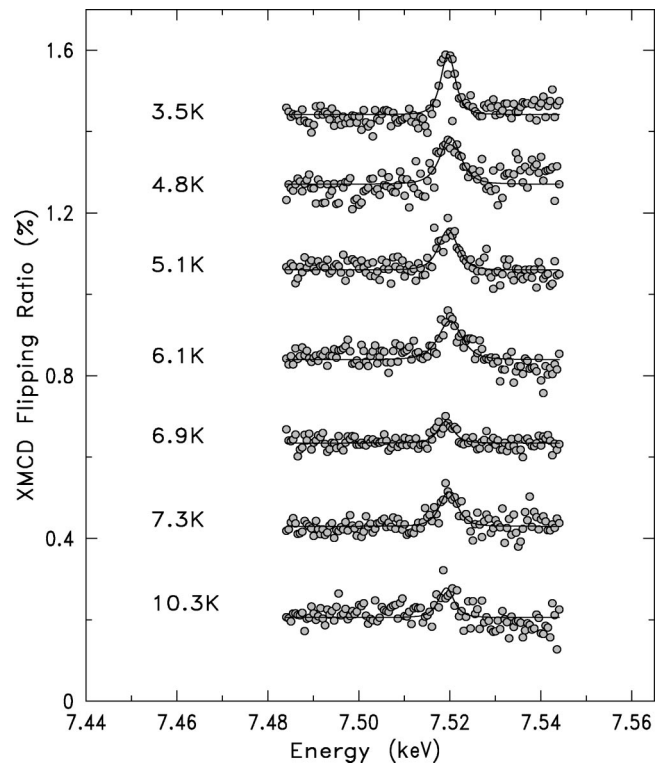

FIG. 2. The dichroic signals plotted for several temperatures at $H=500$ G on $TbNi_2B_2C$. The solid lines are fits to a Lorentzian line shape.

At each temperature and field value, data sets were obtained by reversing the photon helicity for each step in energy, and repeating the whole process after flipping the magnetic field direction. The resulting dichroic signal was obtained from the average value of data obtained for positive and negative field values. One of main advantages of this method is that it compensates for small systematic errors that arise from a slight difference in incident intensity between the left and right circular polarized beams and the residual nonlinearity in the detection system.

As mentioned above, the dichroism measurements were made at the Tb L_{III} edge. In order to estimate the magnitude of the expected signal from the weak ferromagnetic ordering in low external field, data was first taken at $T=3.1$ K in a large applied field of 40 kG. At this field and temperature, bulk magnetization measurements indicate that the ferromagnetic moment is nearly saturated at a value of approximately $7\mu_B$ ($\mu_{sat}\sim 9\mu_B$). In Fig. 1, the absorption edge spectrum as well as the XMCD signal is shown for this temperature and field. The absorption data, $\mu=(1/2)(\mu_{LCP}+\mu_{RCP})=(1/2)[-\log(\delta I_{LCP})-\log(\delta I_{RCP})]$, where $\delta I=I/I_0$, was obtained for both positive (μ_+) and negative (μ_-) external magnetic fields. The average absorption (circles) is displayed in the upper panel of Fig. 1. Similarly, the dichroic signal from the flipping ratio, $(I_{LCP}-I_{RCP})/(I_{LCP}+I_{RCP})$, is shown in the lower panel. At this field and temperature the dichroic signal amounts to approximately 3% of the total absorption.

We now turn to the data obtained from low field measurements ($H=500$ G). The raw dichroic signal at several temperatures is displayed in Fig. 2, along with solid lines that represent fits to a Lorentzian line shape.

The principal result of this experiment is shown in Fig. 3, where the temperature dependence of the intensity of the dichroic signal, obtained from the fits represented in Fig. 2, is plotted. On the same plot, the bulk magnetization data of the same powder sample, measured by a SQUID magneto-

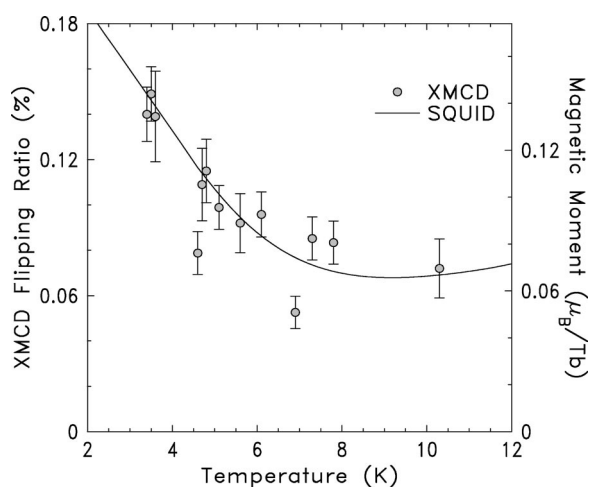

FIG. 3. The dichroic signal taken at $H=500$ G on $TbNi_2B_2C$ is plotted with filled circles. The solid line is the bulk magnetization measurement data on the same powder sample at the same field. The scale for XMCD data is shown to the left while that for the SQUID data are shown to right.

meter at the same field, are also displayed. The only adjustable parameter required to bring the two data sets into coincidence is an overall scale factor. The temperature dependence of the dichroic signal clearly is well described by the temperature dependence of the bulk magnetization data, confirming the onset of ferromagnetic order of the Tb ions below approximately 8 K. These measurements provide direct confirmation of the weak ferromagnetism in $TbNi_2B_2C$ inferred from the bulk susceptibility data.

Due to differences in the radial portion of the transition matrix elements at rare-earth $L_{II,III}$ edges (Ref. 21), a quantitative determination of the actual $5d$ magnetic moments using the sum rule analysis (Ref. 22) is not possible. Nevertheless, it is possible to estimate the size of the $5d$ moment by comparing the spectra with the reported size of the full moment. First, we note that in this measurement, the dichroic signal arises from electric dipole transitions from the Tb $2p_{3/2}$ core level to the $5d$ bands. Therefore, the observed signal arises from the moment induced on the spin polarized $5d$ band. A rough estimate of the ratio of the $5d$ induced moment to $4f$ moment yields a value on the order of $\sim 1/20$ (Ref. 23). The reported weak ferromagnetic component of the moment for $TbNi_2B_2C$ is approximately $0.2\mu_B$. Therefore, the dichroic signal detected in the current measurements arises from an induced $5d$ moment on the order of $0.01\mu_B$.

In order to more closely examine the relationship between the dichroism data and the bulk magnetization data, measurements were also carried out while changing the external magnetic field at a fixed temperature of 3.1 K. The resulting XMCD signal is displayed in Fig. 4 along with the bulk magnetization data from the SQUID measurement. We point out that the same relative scale factor was applied here as was used for Fig. 3. At low fields, good agreement was obtained between the XMCD and SQUID data. At high field, however, there is a noticeable difference between the XMCD and SQUID data. We believe that this difference arises from the fact that the powder used in the XCMD measurements was constrained (bonded to tapes) while the powder sample used in the SQUID measurement was free to rotate in the applied field. At low fields, the difference between the measurements is expected to be negligible, while in high applied field, rotation of the sample grains can yield significantly larger values for the moment.

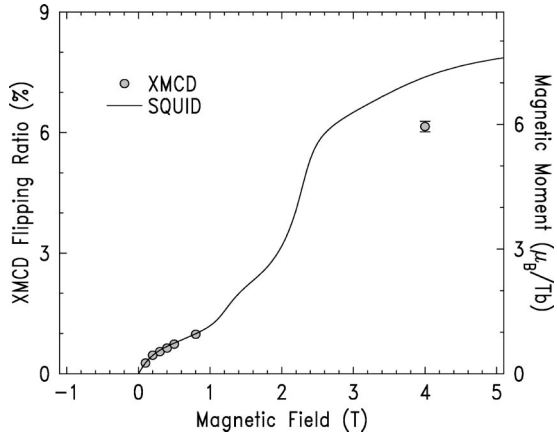

FIG. 4. XMCD and SQUID magnetization data as a function of applied external field at a fixed temperature of 3.1 K on $TbNi_2B_2C$. The scale for the XMCD data is shown to the left while the magnetic moment determined form the SQUID measurements is shown to the right. The smearing of the metamagnetic transitions arises from powder averaging.

Summarizing, the weak ferromagnetism on $TbNi_2B_2C$ has been directly confirmed from the x-ray magnetic circular dichroism measurements at 500 G. A weak ferromagnetic component develops on the Tb ion below ~ 8 K consistent with the bulk susceptibility result.

Ames Laboratory–U.S. DOE is operated by Iowa State University under Contract No. W-7405-Eng-82. The Midwest Universities Collaborative Access Team (MUCAT) sector at the APS is supported by the U.S. Department of Energy, Basic Energy Sciences, Office of Science, through the Ames Laboratory under Contract No. W-7405-Eng-82. Use of the Advanced Photon Source was supported by the U.S. Department of Energy, Basic Energy Sciences, Office of Science, under Contract No. W-31-109-Eng-38.

[1] R. Nagarajan, C. Mazumdar, Z. Hossain, S. K. Dhar, K. V. Gopalakrishnan, L. C. Gupta, C. Godart, B. D. Padalia, and R. Vijayaraghavan, Phys. Rev. Lett. **72**, 274 (1994).

[2] R. J. Cava, H. Takagi, B. Batlogg, H. W. Zandbergen, J. J. Krajewski, W. F. Peck, Jr., R. B. van Dover, R. J. Felder, T. Siegrist, K. Mizuhashi, J. O. Lee, H. Eisaki, S. A. Carter, and S. Uchida, Nature (London) **367**, 146 (1994).

[3] R. J. Cava, H. Takagi, H. W. Zandbergen, J. J. Krajewski, W. F. Peck, Jr., T. Siegrist, B. Batlogg, R. B. van Dover, R. J. Felder, K. Mizuhashi, J. O. Lee, H. Eisaki, and S. Uchida, Nature (London) **367**, 252 (1994).

[4] T. Siegrist, H. W. Zandbergen, R. J. Cava, J. J. Krajewski, and W. F. Peck, Jr., Nature (London) **367**, 254 (1994).

[5] H. Eisaki, H. Takagi, R. J. Cava, B. Batlogg, J. J. Krajewski, W. F. Peck, Jr., K. Mizuhashi, J. O. Lee, and S. Uchida, Phys. Rev. B **50**, 647 (1994).

[6] P. C. Canfield, P. L. Gammel, and D. J. Bishop, Phys. Today **51** (10), 40 (1998).

[7] P. C. Canfield, S. L. Bud'ko, and B. K. Cho, Physica C **262**, 249 (1996).

[8] P. L. Gammel, B. Barber, D. Lopez, A. P. Ramirez, D. J. Bishop, S. L. Bud'ko, and P. C. Canfield, Phys. Rev. Lett. **84**, 2497 (2000).

[9] Z. Q. Peng, K. Klug, and K. Winzer, Physica C **317-318**, 441 (1999).

[10] B. K. Cho, P. C. Canfield, and D. C. Johnston, Phys. Rev. B **53**, 8499 (1996).

[11] B. K. Cho, P. C. Canfield, L. L. Miller, D. C. Johnston, W. P.

Beyermann, and A. Yatskar, Phys. Rev. B **52**, 3684 (1995).

[12] C. Detlefs, D. L. Abernathy, G. Grübel, and P. C. Canfield, Europhys. Lett. **47**, 352 (1999).

[13] C. Detlefs, A. H. M. Z. Islam, T. Gu, A. I. Goldman, C. Stassis, P. C. Canfield, J. P. Hill, and T. Vogt, Phys. Rev. B **56**, 7843 (1997).

[14] C. Song, Z. Islam, L. Lottermoser, A. I. Goldman, P. C. Canfield, and C. Detlefs, Phys. Rev. B **60**, 6223 (1999).

[15] C. Song, D. Wermeille, A. I. Goldman, P. C. Canfield, J. Y. Rhee, and B. N. Harmon, Phys. Rev. B **63**, 104507 (2001).

[16] C. Detlefs, C. Song, S. Brown, A. Kreyssig, P. Thompson, P. C. Canfield, and A. I. Goldman (unpublished).

[17] See, for example, J. C. Lang, *Methods in Materials Research* (Wiley, New York, in press).

[18] P. Dervenagas, J. Zarestky, C. Stassis, A. I. Goldman, P. C. Canfield, and B. K. Cho, Phys. Rev. B **53**, 8506 (1996).

[19] D. R. Sánchez, M. A. C. de Melo, M. B. Fontes, S. L. Bud'ko, E. Baggio-Saitovitch, M. Hillberg, W. Wagener, H.-H. Klauβ, G. H. Walf, and F. J. Litterst, Phys. Rev. B **57**, 10 268 (1998).

[20] K. Hirano, K. Izumi, T. Ishikawa, S. Annaka, and S. Kikita, Jpn. J. Appl. Phys., Part 1 **30**, 407 (1991).

[21] H. König, X. Wang, B. N. Harmon, and P. Carra, J. Appl. Phys. **76**, 6474 (1994).

[22] Paolo Carra, B. T. Thole, Massimo Altarelli, and Xindong Wang, Phys. Rev. Lett. **70**, 694 (1993).

[23] J. Y. Rhee (private communication).